

Enteral Arg-Gln Dipeptide Administration Increases Retinal Docosahexaenoic Acid and Neuroprotectin D1 in a Murine Model of Retinopathy of Prematurity

Lynn Calvin Shaw,¹ Sergio Li Calzi,² Nan Li,³ Leni Moldovan,¹ Nilanjana Sengupta-Caballero,⁴ Judith Lindsey Quigley,¹ Mircea Ivan,⁵ Bokkyoo Jun,⁶ Nicolas G. Bazan,⁶ Michael Edwin Boulton,² Julia Busik,⁷ Josef Neu,³ and Maria B. Grant²

¹Department of Ophthalmology, Indiana University, Indianapolis, Indiana, United States

²Department of Ophthalmology, University of Alabama, Birmingham, Alabama, United States

³Department of Pediatrics, University of Florida, Gainesville, Florida, United States

⁴Department of Anatomy and Biology, Santa Fe College, Gainesville, Florida, United States

⁵Department of Medicine, Indiana University, Indianapolis, Indiana, United States

⁶Department of Ophthalmology, Louisiana State University Eye Center, New Orleans, Louisiana, United States

⁷Department of Physiology, Michigan State University, East Lansing, Michigan, United States

Correspondence: Maria B. Grant, Department of Ophthalmology, University of Alabama at Birmingham, 1670 University Boulevard, Room VH 490, Birmingham, AL 35294, USA; mabgrant@uab.edu.

LCS and SLC contributed equally to the work presented here and should therefore be regarded as equivalent authors.

Submitted: September 23, 2017

Accepted: December 28, 2017

Citation: Shaw LC, Li Calzi S, Li N, et al. Enteral Arg-Gln dipeptide administration increases retinal docosahexaenoic acid and neuroprotectin D1 in a murine model of retinopathy of prematurity. *Invest Ophthalmol Vis Sci*. 2018;59:858–869. <https://doi.org/10.1167/iovs.17-23034>

PURPOSE. Low levels of the long chain polyunsaturated fatty acid (LCPUFA) docosahexaenoic acid (DHA) have been implicated in retinopathy of prematurity (ROP). However, oral DHA suffers from poor palatability and is associated with increased bleeding in premature infants. We asked whether oral administration of the nutraceutical arginine-glutamine (Arg-Glu) could increase retinal DHA and improve outcomes in a mouse model of oxygen-induced retinopathy (OIR).

METHODS. Postnatal day 7 (P7) pups were maintained at 75% oxygen for 5 days and then returned to room air on P12. Pups were gavaged twice daily with Arg-Gln or vehicle from P12 to P17 and eyes were harvested for analysis on P17. Vaso-obliteration and vascular density were assessed on retinal flat mounts and preretinal neovascularization was assessed on retinal cross sections. Retinas were used for measurement of DHA and 10,17S-docosatriene (neuroprotectin D1, NPD1), a key DHA-derived lipid, and for analysis by reverse-phase protein array (RPPA).

RESULTS. With Arg-Gln treatment, retinal DHA and NPD1 levels were increased in OIR pups. Arg-Gln reduced preretinal neovascularization by $39 \pm 6\%$ ($P < 0.05$) relative to vehicle control. This was accompanied by a restoration of vascular density of the retina in the pups treated with Arg-Gln ($73.0 \pm 3.0\%$) compared to vehicle ($53.1 \pm 3.4\%$; $P < 0.05$). Arg-Gln dipeptide restored OIR-induced signaling changes toward normoxia and was associated with normalization of insulin-like growth factor receptor 1 signaling and reduction of apoptosis and an increase in anti-apoptosis proteins.

CONCLUSIONS. Arg-Gln may serve as a safer and easily tolerated nutraceutical agent for prevention or treatment of ROP.

Keywords: nutraceuticals, oxygen-induced retinopathy, retinal proteomic analysis, arg-gln dipeptide, docosahexaenoic acid

Each year more than 30,000 preterm infants worldwide become blind or visually impaired from retinopathy of prematurity (ROP).¹ In the 1940s the “first ROP epidemic” was observed due to the prevalent use of unrestricted oxygen supplementation for treatment of infants with respiratory distress. High oxygen levels inhibit blood vessel growth and induce degeneration of existing microvasculature in the developing retina. The return to normal oxygen levels, when the infant’s respiratory status improves, is misinterpreted by the retina as a state of relative hypoxia. This change initiates neovascularization that leads to visual impairment and ROP. The second “ROP epidemic” transpired in affluent countries in the 1970s and was due to the improved survival of the lower-gestational-age (GA) infants.² In the early 1990s, a “third”

epidemic was due to increased survival of premature infants in middle-income countries including Asia and Latin America where the incidence of blindness/severe visual impairment became higher than in highly industrialized countries such as the United States. Despite current therapeutic strategies, ROP remains a prevalent cause of potentially preventable visual impairment and blindness in childhood.

The concept of combining arginine and glutamine as a dipeptide (Arg-Gln) stems from two lines of reasoning. The Arg-Gln combination obviates the decomposition of aqueous glutamine into the cyclic product associated with ammonia liberation and improves the solubility in water.^{3,4} Second, dipeptides are better absorbed than single amino acids.⁴

Dipeptidases cleave Arg-Gln once the peptide enters the circulation.⁵

Stress, common in premature infants in neonatal intensive care units, can induce amino acid deprivation, specifically arginine and glutamine deficiency.^{6,7} Deprivation of retinal glutamine increases the expression of VEGF,⁸⁻¹⁰ a potent retinal angiogenic factor. Supplementation of glutamine in low-birth-weight infants is safe as shown by multicenter trials using either intravenous or enteral glutamine supplementation.^{6,11} Arginine supplementation in low-birth-weight infants results in a reduction in necrotizing enterocolitis likely due to improved intestinal blood flow mediated by increased local nitric oxide production.¹² In this study, we sought to determine whether Arg-Gln has beneficial effects when given by the enteral route as would occur for use in infants and, if so, the potential mechanism for this effect. We found that enteral treatment of dipeptide prevented high oxygen-induced vaso-obliteration and pathologic neovascularization while promoting vascular regrowth in the oxygen-induced retinopathy (OIR) model. These changes were accompanied by an increase in retinal levels of docosahexaenoic acid (DHA), the major omega-3 polyunsaturated fatty acid (PUFA) in the retina that plays a significant role in maintaining the health of the retina.

MATERIALS AND METHODS

Mouse Model of Oxygen-Induced Retinopathy

All animals were treated in accordance with the ARVO Statement for the Use of Animals in Ophthalmic and Vision Research. The Institutional Animal Care and Use Committees of the University of Florida and of Indiana University approved animal procedures. C57BL6/J timed-pregnant mice were purchased from Jackson Laboratories (Bar Harbor, ME, USA). The mice were housed in the University of Florida Health Science Center Animal Care facilities or in the Indiana University Laboratory Animal Resource Center at Indiana University-Purdue University (Indianapolis campus). In the neonatal mouse model of OIR, 7-day-old mice were placed with their nursing dams in a 75% oxygen atmosphere for 5 days. On postnatal day 12 (P12) and continuing through postnatal day 17 (P17), mouse pups received twice-daily gavage feedings (20 μ L). The types of gavage feedings included vehicle (0.9% sodium chloride), Arg-Gln dipeptide (1, 2.5, or 5 g/kg body weight per day as a hydrochloride salt; Bachem, Babendorf, Switzerland), or the ethyl ester form of DHA (2.5 g/kg body weight per day). For each type of gavage feeding, we used three litters of pups. On average, a litter consists of six pups. Therefore, each data point represents a minimum of one eye each from six pups and was repeated three times. On the fifth day after return to normoxia (P17), the animals were euthanized. Additional controls included nongavaged pups that underwent the OIR model and pups maintained at normoxia.

Selected eyes were removed and fixed in 4% paraformaldehyde, embedded in paraffin, and sectioned as previously described.⁵ Other eyes were prepared for quantitative retinal flat-mount analysis. These mice at the time of euthanasia were perfused with FITC-labeled dextran (MWt = 2×10^6) (Sigma-Aldrich Corp., St. Louis, MO, USA) to visualize the vasculature. Eyes were then enucleated, incubated in 4% formaldehyde, and then in PBS. Neural retina was dissected from the RPE-choroid-sclera complex. Four to seven radial cuts were made in the retina to allow the retina to lie flat for imaging using confocal microscopy (MRC-1024 Confocal Laser Scanning System; Bio-Rad, Hercules, CA, USA).

Determination of Preretinal Neovascularization in the OIR Model

Serial sections (6 μ m) of whole eyes were cut sagittally, and approximately 150 serial sections were cut from each eye. Between two and four sections on each side of the optic nerve, 30 to 90 μ m apart, were counted for neovascularization as described by Smith et al.¹³ We excluded cross sections that included the optic nerve because of the normal vessels emanating from the optic nerve. Vascular cell nuclei, identified under light microscopy with hematoxylin staining, were considered to be associated with new vessels if they were found on the vitreal side of the internal limiting membrane. Masked observers counted preretinal nuclei. Efficacy of treatment was calculated as the percentage of average of nuclei per section in the eyes of treated animals versus control animals.⁵

Determination of Retinal Vaso-Obliteration in the OIR Model

The FITC-labeled dextran retinal flat mounts were used to determine the relative levels of vaso-obliteration. TIF images of the retinal flat mounts were used to determine the areas of the retina and of the vaso-obliterated regions using ImageJ.¹⁴

Determination of Retinal Vascular Density in the OIR Model

The FITC-labeled dextran retinal flat mounts were used to determine the relative levels of vascular density. The retina was divided arbitrarily into 12 sectors, akin to the 12 hours of a clock. Images were taken in 10 of the 12 sectors. TIF images of the retinal flat mounts were used to segregate each retina into central retina, midperipheral retina, and peripheral retina regions. Each image was overlaid with a grid of equally spaced squares using Adobe Photoshop V5.0 (Adobe Systems, San Jose, CA, USA) with the number of grids for each region ranging from two to six.¹⁵ Fields of view selected for analysis in peripheral retinas included regions of capillary-sized vessels directly adjacent to radial arterioles, whereas areas selected for analysis in central and midperipheral retinas included the radial arterioles. The actual grid was superimposed onto each image. The intersections of the grid with the dextran-labeled vasculature were shown as yellow dots. The mean vascular density incidence was determined for each area and compared to its control. The data are presented as means \pm SD.¹⁶

Tissue Fatty Acid Analysis by Reverse-Phase-High-Performance Liquid Chromatography (RP-HPLC)

An aliquot of total lipids from neural retina was saponified (0.4 N KOH in 80% methanol, 50°C for 1 hour). Saponified fatty acids were acidified and extracted with diethyl ether according to Wang et al.¹⁷ and stored in methanol containing 1 mM butylated hydroxytoluene. Saponified free fatty acids were fractionated and quantitated by RP-HPLC using a YMC J-Sphere (ODS-H80) column (Allentown, PA, USA) and a sigmoidal gradient starting at 86.5% acetonitrile + acetic acid (0.1%) (Sigma-Aldrich Corp.) and ending at 100% acetonitrile + acetic acid (0.1%) over 50 minutes with a flow rate of 1.0 mL/min using a Waters Corporation 600 controller (Milford, MA, USA). Fatty acids were introduced to the HPLC by injection in methanol and detected using ultraviolet absorbance and evaporative light scatter as previously described.¹⁷ Authentic fatty acid standards (Nu-Chek Prep, NIC, Elysian, MN, USA) were used to generate calibration curves for verification and quantification of fatty acids.

Neuroprotectin D1 (NPD1) Analysis

Neural retinas were homogenized with glass homogenizer in cold methanol (total of 3 mL). After the homogenization, 6 mL cold CHCl_3 was added. Internal standard mixture (AA-d8, EPA-d5, LTB4-d4, 15HETE-d8, and PGD2-d4) (Cayman Chemical, Ann Arbor, MI, USA) was added, then sonicated. Samples were centrifuged and pellets were collected for protein measurement. Supernatant was mixed with pH 3.5 water, and the pH of aqueous phase was adjusted. After discarding upper phase, the bottom phase was dried and resuspended in 40 μL methanol:H₂O = 1:1 for mass spectrometry. Xevo TQ-S equipped with Acquity I Class UPLC (Waters Corporation) was used for lipidomics. Acquity UPLC HSS T3 1.8- μm 2.1 \times 50-mm column was used for separation of fatty acids and their derivatives. Forty-five percent of solvent A (H₂O + 0.01% acetic acid) and 55% of solvent B (methanol + 0.01% acetic acid) with 0.4 mL/min flow were used initially, followed by gradient to 15% of solvent A for the first 10 minutes, then gradient to 2% of solvent A at 18 minutes. Two percent of solvent A ran for 25 minutes, then gradient back to 45% of solvent A for re-equilibration for 30 minutes. The capillary voltage was -2.5 kV, desolvation temperature at 600°C , desolvation gas flow at 1100 L/h, cone gas at 150 L/h, and nebulizer pressure at 7.0 bar with the source temperature at 150°C . MassLynx 4.1 software (Waters Corporation) was used for operation and recording of the data. Mass spectrometry data were analyzed and calculated with Excel (Microsoft Corp., Redmond, WA, USA).

Proteomic Analysis

For protein expression assays, retinas from each pup were disrupted in the TissueLyser LT (Qiagen, Germantown, MD, USA) in 200 μL lysis buffer provided by the Functional Proteomics Reverse Phase Protein Array (RPPA) Core Facility (M.D. Anderson Cancer Center, Houston, TX, USA): 1% Triton X-100, 50 mM HEPES pH 7.4, 150 mM NaCl, 1.5 mM MgCl_2 , 1 mM EGTA, 100 mM NaF, 10 mM Na pyrophosphate, 1 mM Na_3VO_4 , 10% glycerol, and freshly added protease and phosphatase inhibitors (Roche Diagnostics Corporation, Indianapolis, IN, USA). After pelleting the debris, the protein concentration was determined with the Pierce BCA microplate procedure (Thermo Fisher Scientific, Waltham, MA, USA) on a Synergy H1 plate reader (BioTek, Winooski, VT, USA), adjusted to ~ 1 $\mu\text{g}/\mu\text{L}$ and sent to RPPA Core for proteomic analysis using their standard procedures (<https://www.mdanderson.org/research/research-resources/core-facilities/functional-proteomics-rppa-core.html>; in the public domain).

Statistical Analysis

All results are expressed as the mean \pm SEM. The values were processed for statistical analyses by ANOVA followed by *t*-test assuming unequal variances using statistical analysis software (SPSS, Chicago, IL, USA). Differences were considered statistically significant at $P < 0.05$. The number of animals is indicated in the figure legends, with a minimum of five mice per group.

RESULTS

The Arg-Gln Dipeptide Significantly Reduced Preretinal Neovascularization in the OIR Mouse Model

Gavage with the Arg-Gln dipeptide showed a dose-dependent reduction in preretinal neovascularization similar to the intraperitoneal injection of Arg-Gln⁵ with the maximum dose of 5 g/kg body weight/day, resulting in the largest reduction in preretinal neovascularization ($39 \pm 6\%$; $P < 0.05$ relative to

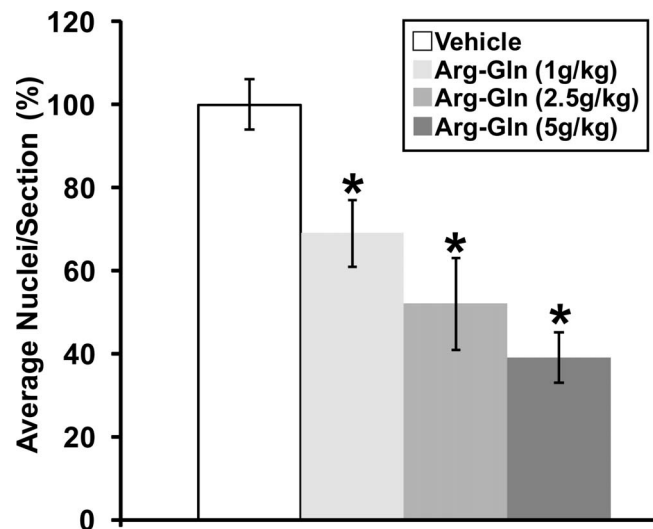


FIGURE 1. Arg-Gln dipeptide administered by gavage reduces preretinal neovascularization in the OIR mouse model. Graphical summary of the analysis of preretinal neovascularization levels in the OIR mouse model following gavage treatments. The numbers in brackets refer to gavage doses in g/kg body weight/day. *Indicates P values < 0.05 compared to vehicle ($n = 11$ for vehicle, $n = 18$ for dipeptide concentration, $n = 6$ for normoxia).

vehicle control) (Fig. 1). The maximal dose of 5 g/kg per day was used in all subsequent studies.

In this model, body weight can affect the formation and regression of retinal neovascularization.¹⁸ However, no difference was noted as the average weight of the OIR controls (pups treated with vehicle) was $7.16 \text{ g} \pm 0.4$, while the average weight of the pups in the experimental cohorts was $6.62 \text{ g} \pm 0.8$ ($P = 0.198$).

Arg-Gln Dipeptide Significantly Reduced Vaso-Obliteration in the OIR Mouse Model

Treatment with the Arg-Gln dipeptide showed a significant reduction in vaso-obliteration compared to vehicle-treated mice (Fig. 2). The average level of vaso-obliteration in vehicle-treated mice was $28 \pm 4\%$ (Fig. 2B) when compared to normoxic pups (Fig. 2A), whereas treatment with the Arg-Gln dipeptide significantly reduced vaso-obliteration to $6.7 \pm 5\%$ ($P = 0.03$; Fig. 2C). Areas outlined in yellow represent areas of vaso-obliteration. Figure 2D shows the graphical summary of these results.

Retinal Vascular Density in the OIR Model Is Significantly Higher in Mice Treated With the Arg-Gln Dipeptide

Retinal flat mounts from FITC-dextran-perfused mice are shown in Figures 3A through 3C. The OIR vehicle-treated pups demonstrated a large area with loss of vasculature (Fig. 3A) compared to the normoxia control (Fig. 3C), pups not undergoing OIR. Treatment with the dipeptide markedly increases vascular regrowth (Fig. 3B). A graphical summary of all the vascular density area represented as a percent of normoxia control demonstrates that Arg-Gln had a beneficial effect in restoring retinal vascular density when compared to vehicle controls (Fig. 3D). This effect is most evident in the central retina where the majority of vessel loss occurs in the OIR model (central: vehicle = $30.8 \pm 22.7\%$, P value = 0.0005, Arg-Gln = $79.3 \pm 6.0\%$, P value = 0.02; midperiphery: vehicle = $68.4 \pm 3.8\%$, P value = 0.002, Arg-Gln = $102.6 \pm 2.8\%$, P value

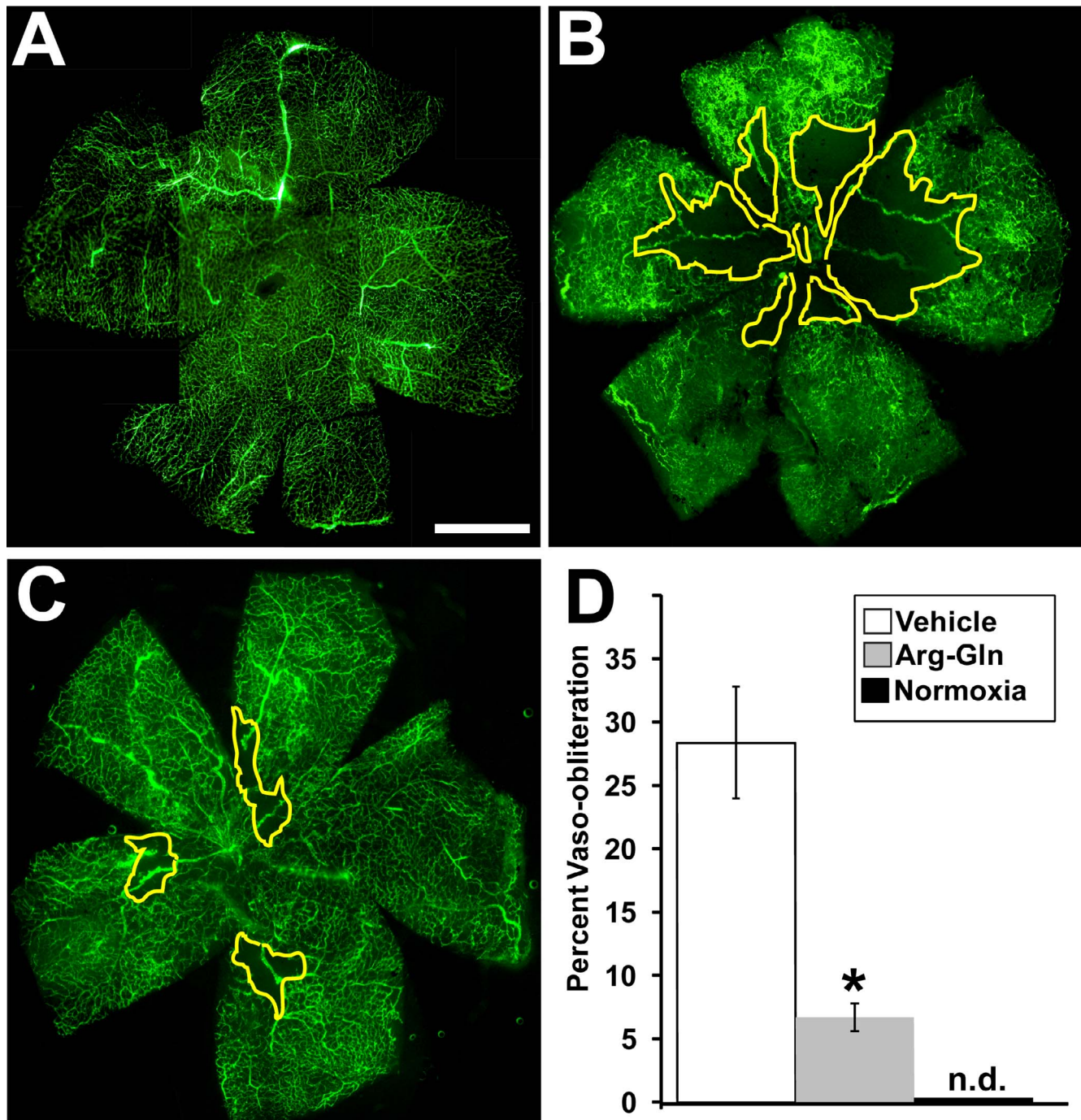


FIGURE 2. Arg-Gln dipeptide administered by gavage reduces vaso-obliteration in the OIR mouse model. Representative retinal flat mounts from FITC-dextran-perfused mice from (A) normoxic mouse pups (P17) $n = 6$, (B) ROP mouse pups treated with the vehicle (P17) $n = 11$ ($P = 0.03$), (C) dipeptide-treated pups (P17) $n = 9$ ($P = 0.02$). (D) Graphical representation of all results (n.d., not detected). The yellow lines delineate the areas of retinal vaso-obliteration in (B, C). Scale bar: 1 mm.

$= 0.4$; periphery: vehicle = $81.7 \pm 5.3\%$, P value = 0.01, Arg-Gln = $102.3 \pm 3.2\%$, P value = 0.5).

Retinal DHA and NPD1 Levels Are Restored to Normal in the OIR Model by Treatment With Arg-Gln Dipeptide

In the neural retina of the mouse pups, we examined whether the dipeptide could change levels of DHA, the omega-3 PUFA that is concentrated in phospholipids of synaptic membranes,

retinal pigment epithelium cell (RPE), and photoreceptors. In normoxic mice the molar percentage (mol%) of DHA in the neural retina was $25.4 \pm 3.2\%$ (Fig. 4A). In the OIR model, mice treated with vehicle demonstrated a significantly lower mol% of DHA of $16.7 \pm 2.6\%$ ($P < 0.05$). DHA levels were restored to normoxic levels by treatment with Arg-Gln dipeptide ($23.4 \pm 1.6\%$; $P > 0.2$, when compared to normoxic). DHA mediates its protective effects in part by increasing generation of neuroprotectants.¹⁹ A specific mediator generated from DHA that contributes largely to its

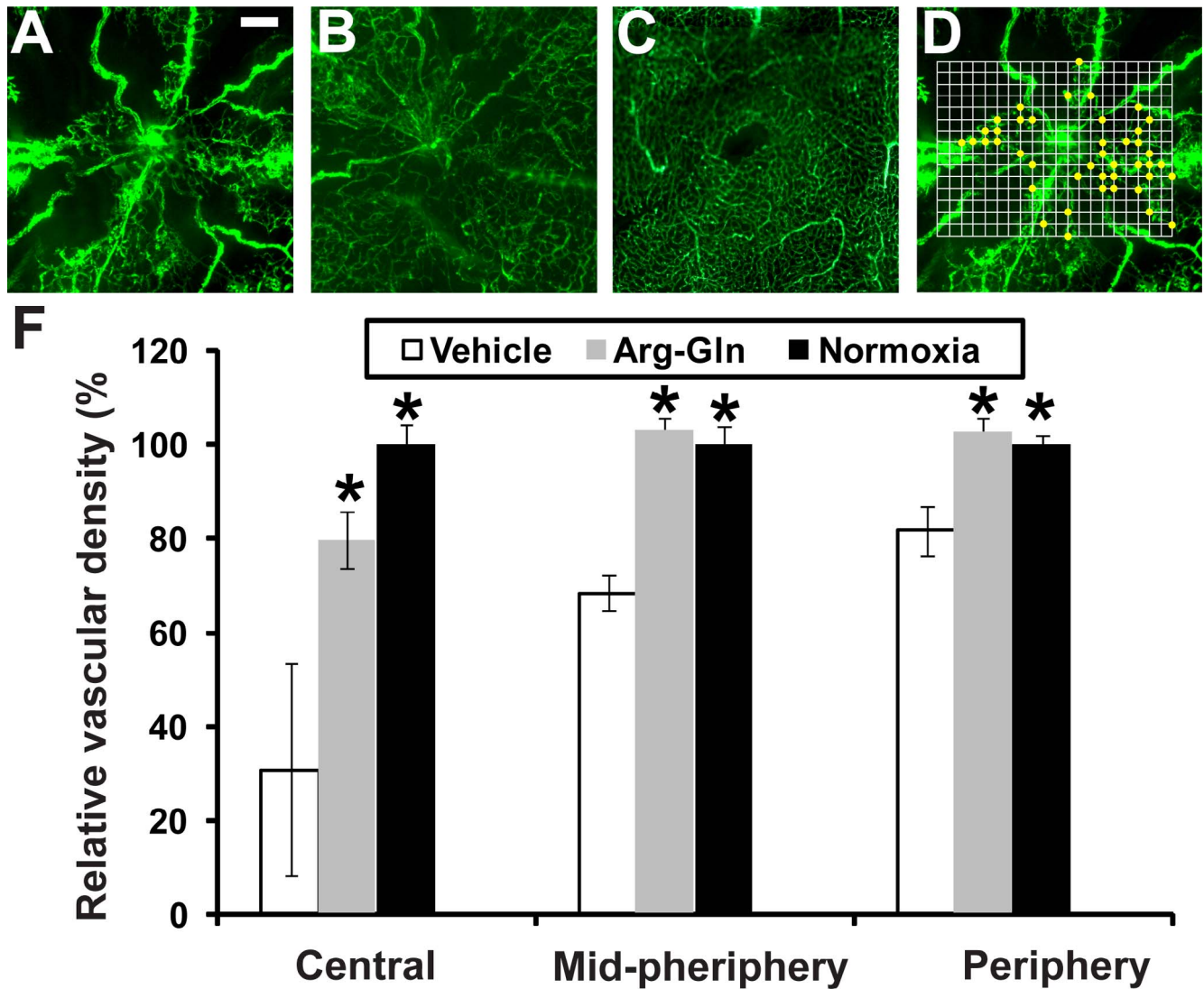


FIGURE 3. The Arg-Gln dipeptide administered by gavage promotes retinal blood vessel regrowth in the OIR model. (A–C) Retinal flat mounts from FITC-dextran-perfused mice. (A) Representative retinal flat mount from mouse pup undergoing OIR model and treated with vehicle given by gavage ($n = 10$). (B) Representative retinal flat mount from mouse pup undergoing OIR model and treated with the Arg-Gln dipeptide ($n = 7$). (C) Representative retinal flat mount from healthy control mouse maintained at room air and euthanized at P17 ($n = 6$). (D) An example of how vascular density is determined. The actual grid was superimposed onto each image. The intersections of the grid with the dextran-labeled vasculature were shown as *yellow dots*. (E) Graphical summary of all the vascular density data from all three cohorts of mice. *Indicates that P values compared to vehicle are < 0.05 . Scale bar: 0.2 mm.

biological significance in the retina is 10,17S-docosatriene (neuroprotectin D1, NPD1). In normoxic (non-OIR) mice, the level of NPD1 in the neural retina was set at $100 \pm 83\%$ (Fig. 4B). The level of NPD1 in OIR mice was $356 \pm 141\%$ ($P < 0.05$). NPD1 level in Arg-Gln-treated mice was $3150 \pm 340\%$ ($P < 0.05$).

DHA Supplementation of ROP Pups Results in Reduction of Preretinal Neovascularization, Reduction in Vaso-Obliteration, and Increase in Retinal NPD1 levels

We next asked whether directly supplementing mouse pups with DHA by gavage administration would result in a similar beneficial effect as we observed with the dipeptide. Treatment with DHA shows a reduction in preretinal neovascularization of $49 \pm 4\%$ ($P < 0.05$) (Fig. 5A).

DHA treatment resulted in a reduction in vaso-obliteration (representative retinal flat mount in Fig. 5B; graphical summary in Fig. 5C) compared to vehicle-treated control (Fig. 2A) and comparable to dipeptide-treated mice (Fig. 2C). The average level of vaso-obliteration in vehicle-treated mice was $28 \pm 8\%$ whereas treatment with DHA resulted in a significant reduction in vaso-obliteration to $6.3 \pm 1.32\%$ ($P = 0.02$). There was no significant difference in the level of vaso-obliteration between the mice treated with Arg-Gln ($6.7 \pm 1.2\%$) or DHA ($6.3 \pm 1.32\%$). However, unlike the dipeptide, DHA did not have a beneficial effect in restoring retinal vascular density when compared to vehicle controls (Figs. 5D, 5E; central: vehicle = $30.8 \pm 22.7\%$, DHA = $46.4 \pm 13.7\%$, P value = 0.06 ; midperiphery: vehicle = $68.4 \pm 3.8\%$, DHA = $78.6 \pm 5.7\%$, P value = 0.1 ; periphery: vehicle = $81.7 \pm 5.3\%$, DHA = $84.9 \pm 4.6\%$, P value = 0.4).

In normoxic mice the mol% of DHA was $25.4 \pm 3.2\%$ (Fig. 5F). In the OIR model, mice treated with vehicle demonstrated

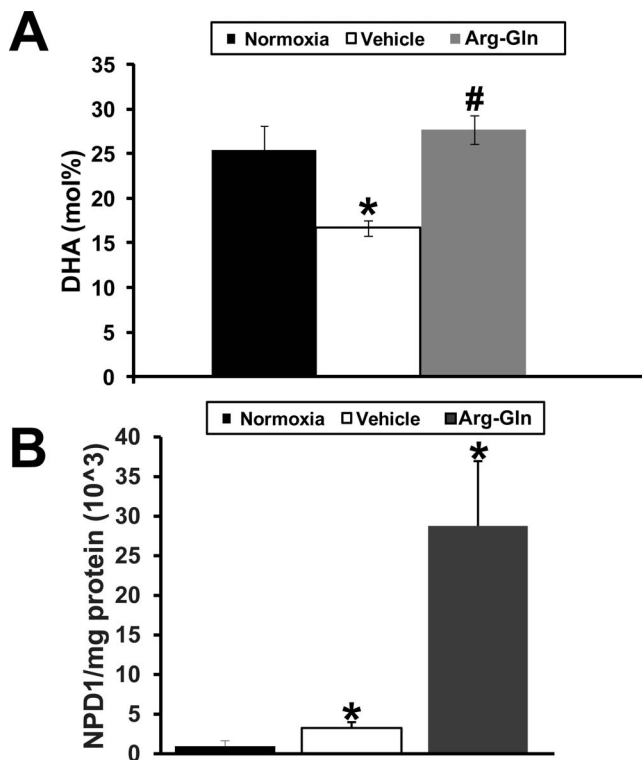


FIGURE 4. Arg-Gln dipeptide elevates retinal DHA and NPD1 levels in the OIR mouse model. Retinas from normoxic and OIR mice treated as indicated. **(A)** The mol% of DHA was determined relative to total fatty acids by HPLC in whole retinas ($n = 6$). **(B)** The level of retinal NPD1 as determined by mass spectrometry analysis. The level of NPD1 relative to total milligrams of retinal protein is shown. * $P < 0.05$ when compared to normoxia; # $P > 0.2$ when compared to normoxia and $P < 0.05$ when compared to vehicle.

a significantly lower mol% of DHA of $16.7 \pm 2.6\%$ ($P < 0.05$). However, DHA levels were restored to normoxic levels by treatment with DHA as expected ($27.5 \pm 2.3\%$; $P = 0.2$, when compared to normoxic). In normoxic (non-OIR model) mice the level of NPD1 was set at $100 \pm 83\%$ (Fig. 5G). The level of NPD1 in OIR mice was $356 \pm 141\%$ ($P < 0.05$). NPD1 level in DHA-treated mice was $2516 \pm 340\%$ ($P < 0.05$).

Arg-Gln Dipeptide Restored OIR-Induced Signaling Changes Toward Normoxia in P17 Mouse Pup Retinas

Our studies thus far would suggest that the beneficial effects of the dipeptide are associated with increases in retinal DHA and NPD1. To better establish the mechanisms mediating these effects, we performed signaling arrays (Figs. 6A, 6B). The Table lists the significantly up- and downregulated proteins in neural retinas of OIR model pups compared to age-matched pups raised in normoxia. The OIR model induces proteins that mediate proliferation (IGF-receptor b [IGFRb], insulin receptor b [IR-b], Src, and PI3K) and other proteins associated with apoptosis (JNK2, programmed cell death protein 4, RPA32, and BIM). The model increases the autophagy protein, LC3A, and two proteins implicated in retinal vascular leakage (connexin-43 and serine-protein kinase ATM). The model is associated with downregulation of proteins that are known to be protective against DNA damage and cellular stress (AKT1 kinase, HSP27, and HSP70). Treatment with the Arg-Gln dipeptide resulted in normalization of upregulated levels of connexin-43, Src, and IGFRb and restoration of downregulated

levels of caveolin-1, Axl, Bcl-xl, Mnk1, and WIPI2 toward normal (shown in green in Table).

DHA treatment resulted in a reduction of the autophagy protein LC3A toward normoxia and reductions of phosphoribosylaminoimidazole succinocarboxamide synthase (PAICS) and RPA32 and increases of E-cadherin and p70-S6K1 toward normoxia levels (shown in blue in Table).

Some retinal proteins upregulated by the OIR model (XRCC1, collagen VI, JNK2, ATM, IR-b, Pdcd4, and PI3K) were downregulated by either the dipeptide or DHA. Some proteins downregulated by the OIR model were increased by both the dipeptide and DHA, including Akt, eEF2K, HSP27, HSP70, MSH6, c-Jun, and merlin (shown in beige in Table). The complete series of proteins examined in the retinas of the OIR pups are shown in Figure 6 (higher expression in Fig. 6A or lower expression Fig. 6B).

DISCUSSION

Currently, there are limited safe pharmacologic options for the treatment of ROP. Discovery of a new, easily affordable treatment and preventative strategy, such as the Arg-Gln dipeptide described in this study, may be a highly relevant approach of global interest. Treatments such as systemic administration of propranolol or ocular administration of anti-VEGF are associated with side effects in premature infants.²⁰ Intravenous propranolol has been associated with arrhythmias.²¹ Intraocular anti-VEGF has been associated with systemic inhibition of VEGF for up to 8 weeks after a single injection.²² The effects of systemic VEGF inhibition on other developing vascular beds such as the lungs are unknown.

Treatment failure and adverse events such as persistent avascular retina, retinal detachment, and blindness have also been reported.^{20,23–25} While studies have aimed to decrease intraocular concentrations of growth factors such as VEGF levels, other treatment strategies have supported the need to safely increase levels of the growth factor, insulin-like growth factor-1 (IGF-1), to improve VEGF signaling and promote physiological revascularization in premature infants²⁶ in need of oxygen therapy.

Our studies support that the Arg-Gln dipeptide serves to increase endogenous DHA production in a safe and beneficial manner for premature infants. Massive maternal-fetal transfer of long chain polyunsaturated fatty acids (LCPUFAs) occurs during the third trimester of a healthy pregnancy; thus preterm infants do not receive sufficient amounts of DHA to synthesize PUFAs through the series of $\Delta 5$ -desaturase ($\Delta 5D$), $\Delta 6$ -desaturase ($\Delta 6D$), or $\Delta 9$ -desaturase ($\Delta 9D$) and elongation (Elovl-2, -5, and -6) reactions. Using the identical model of OIR employed in the current study, Connor et al.²⁷ demonstrated that supplementation of the diets of nursing dams with omega-3 PUFAs resulted in decreased levels of pathologic angiogenesis.

Administration of fish oil to preterm infants from the first day of life showed a significantly lower incidence and severity of ROP and risk of laser therapy in the treated group.²⁸ A randomized controlled trial²⁸ demonstrated that either breast milk or formula supplemented with LCPUFAs when given to premature infants prevented DHA levels from declining in blood, allowing generation of cerebral phospholipids needed for maturation of visual acuity and cognitive function.²⁹

In agreement with Connor et al.,²⁷ we show that DHA levels are reduced in the retina in the OIR pups from 25 mol% in normal pups to 17 mol% at P17, and this lower level of retinal DHA levels is associated with an increase in central retinal obliteration and an increase in neovascularization. The retina contains the highest concentration of DHA of all tissues, where it is cytoprotective and in particular neuroprotective.^{30–33} The

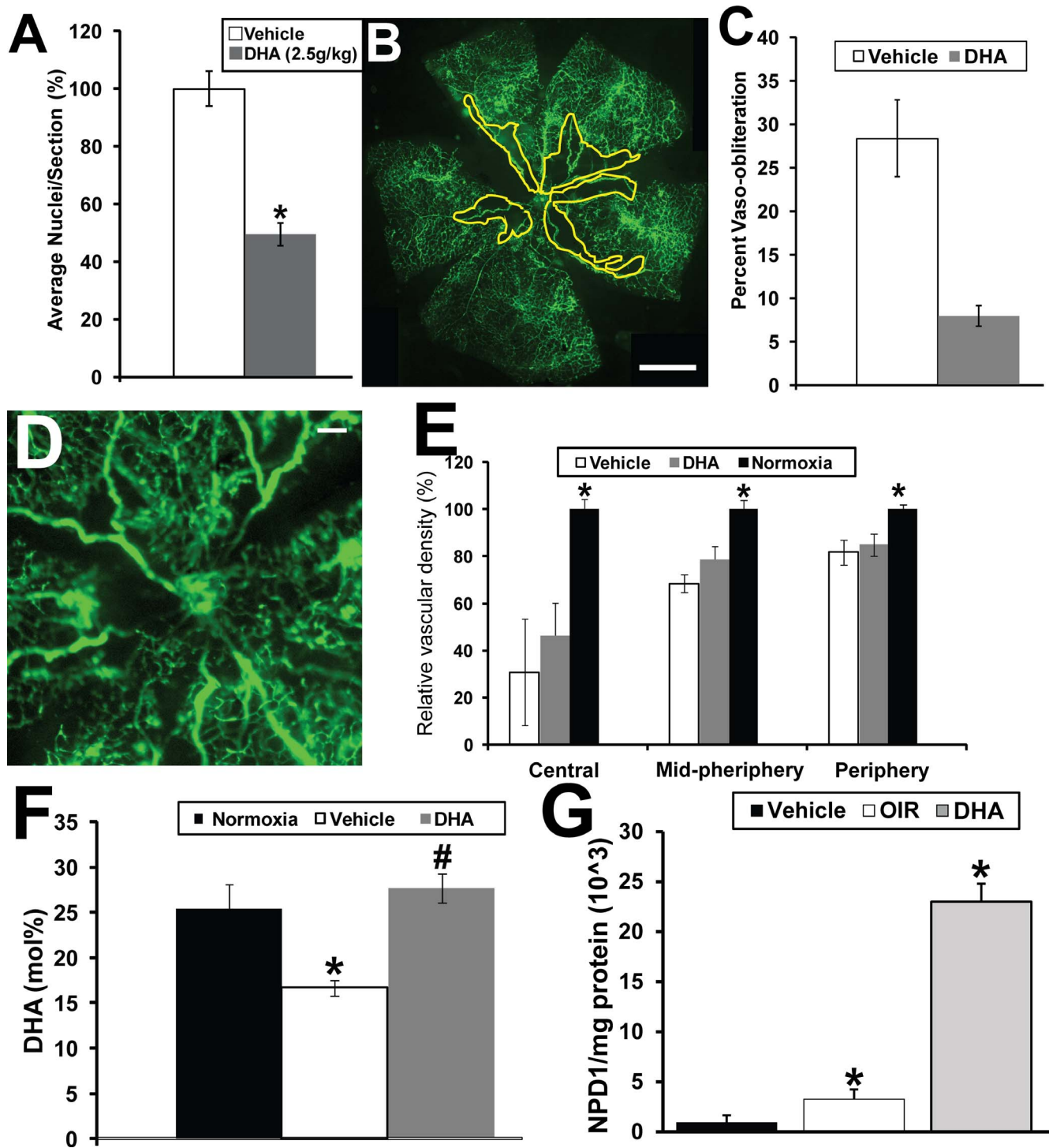


FIGURE 5. DHA given by gavage reduces preretinal neovascularization and vaso-obliteration but not vascular density in the OIR mouse model. (A) Graphical summary of the analysis of preretinal neovascularization levels in the OIR mouse model following gavage treatments of DHA ($n = 15$) and vehicle. *Indicates P values < 0.05 compared to vehicle. (B) Representative retinal flat mount from FITC-dextran-perfused mouse undergoing OIR and treated with vehicle. Scale bar: 1 mm. (C) Graphical representation of reduction in vaso-obliteration with treatment of pups with DHA via gavage in the OIR model. *Indicates a P value < 0.05 ($n = 8$). #Indicates a P value > 0.05 ($n = 8$). (D) Representative retinal flat mount from FITC-dextran-perfused DHA-treated OIR mouse showing reduced vascular density suggesting that, unlike the dipeptide-treated OIR mice, DHA does not promote vascular regrowth. Scale bar: 0.2 mm. (E) Graphical summary of the analysis of retinal vascular density in the mice undergoing OIR and gavage treatments with vehicle or DHA ($n = 5$) compared to mice maintained under normoxia. *Indicates P values < 0.05 compared to normoxia. (F) Retinal DHA levels in the pups receiving DHA or vehicle compared to normal room air controls. (G) Retinal NPD1 levels in the pups receiving DHA ($n = 6$) or vehicle ($n = 6$) compared to normal room air controls ($n = 6$). The yellow line in (B) delineates the areas of retinal vaso-obliteration. *Indicates P values < 0.05 compared to normoxia.

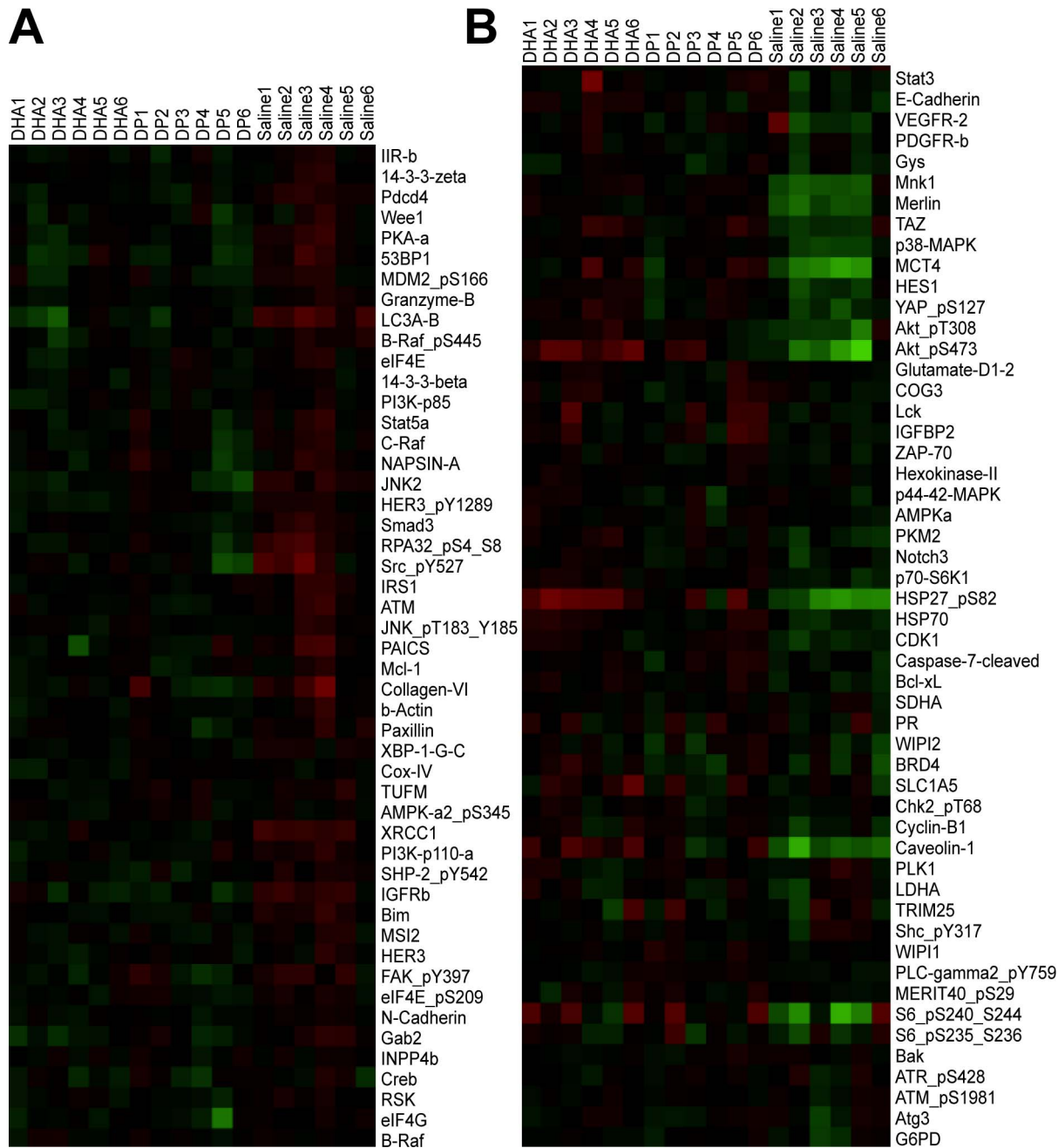


FIGURE 6. Cluster of proteins that have altered expression in the OIR model. Retinas of cohorts of DHA-treated ($n = 6$) and Arg-Gln-treated OIR mice are compared to saline-injected OIR pups ($n = 6$). (A) Proteins with higher expression in OIR control (saline-injected pups) compared to both Arg-Gln and DHA treatments, which reduce their expression often more in the Arg-Gln group. *Red*: upregulation; *green*: downregulation. (B) Proteins that have lower expression in OIR control (saline-injected pups) while both Arg-Gln and DHA treatments increase their expression, often more in the DHA group. *Red*: upregulation; *green*: downregulation.

high concentration of DHA in membranes of retinal photoreceptors and neurons is indicative of the importance of DHA in membrane-associated functions. DHA is required for the regeneration of rhodopsin and signal transduction in photoreceptor cells.³⁴⁻³⁷ LCPUFAs derived from DHA are required to maintain the highly curved edges of the photoreceptor discs of the outer segment.³⁸⁻⁴⁰ Not surprisingly, levels of DHA are reduced in not only ROP but also in other ocular diseases such as diabetic retinopathy^{41,42} and age-related macular degeneration.⁴³⁻⁴⁶ When considering DHA therapeutically, several limitations exist. DHA is unstable and has a short shelf life. Furthermore, it is not tolerated by some infants, resulting in

reduced feeding because of difficulty in camouflaging the flavor of DHA. Use of DHA has been associated with increased bleeding at the time of teething.⁴⁷

Intraperitoneal injection of the Arg-Gln dipeptide at 5 g/kg body weight reduced neovascularization by $52 \pm 6\%$ ⁵ whereas oral Arg-Gln dipeptide reduced neovascularization by $61 \pm 6\%$ as would be the preferred route in preterm infants. Feeding the OIR pups with Arg-Gln dipeptide restores DHA to normoxic levels by P17. The magnitude of the dipeptide effect was similar to that of direct DHA supplementation, and both the dipeptide and the DHA supplement restored retinal DHA levels

TABLE. Proteomic Analysis of Retina From Normoxia Pups, OIR Pups, and Pups Undergoing Gavage With the Arg-Gln Dipeptide or DHA

Proteins Upregulated in OIR							
Protein	Normoxia	OIR	P Value	DP	P Value	DHA	P Value
Conexin-43	100 ± 7	132 ± 7	0.04	118 ± 8	0.13	122 ± 4	0.03
Src	100 ± 2	115 ± 4	0.024	100 ± 3	0.46	106 ± 1	0.02
IGFRb	100 ± 1	110 ± 2	0.006	98 ± 1	0.7	100 ± 2	0.47
LC3A	100 ± 4	129 ± 2	0.0003	113 ± 3	0.012	109 ± 3	0.08
PAICS	100 ± 0.4	111 ± 2	0.015	104 ± 2	0.084	101 ± 2	0.41
RPA32	100 ± 1	108 ± 2	0.04	98 ± 2	0.26	98 ± 1	0.8
XRCC1	100 ± 1	114 ± 2	0.0012	104 ± 1	0.01	104 ± 1	0.04
Collagen VI	100 ± 2	111 ± 3	0.045	101 ± 3	0.4	102 ± 1	0.25
JNK2	100 ± 1	111 ± 1	0.0006	101 ± 3	0.45	101 ± 1	0.2
ATM	100 ± 1	110 ± 2	0.008	104 ± 1	0.017	105 ± 1	0.005
IR-b	100 ± 0.1	108 ± 1	0.0002	105 ± 2	0.05	104 ± 1	0.0056
Pdcd4	100 ± 0.3	109 ± 1	0.0004	101 ± 1	0.25	101 ± 1	0.14
PI3K	100 ± 1	106 ± 1	0.011	102 ± 1	0.23	100 ± 1	0.48
Proteins Downregulated in OIR							
Protein	Normoxia	OIR	P Value	DP	P Value	DHA	P Value
Caveolin-1	100 ± 2	89 ± 6	0.03	108 ± 3	0.002	118 ± 5	0.08
Axl	100 ± 0.2	94 ± 2	0.04	99 ± 2	0.4	95 ± 2	0.09
Bcl-xl	100 ± 1	90 ± 1	0.001	94 ± 1	0.13	95 ± 1	0.02
Mnk1	100 ± 2	90 ± 4	0.049	103 ± 1	0.098	104 ± 1	0.051
WIPI2	100 ± 1	93 ± 2	0.03	96 ± 3	0.17	96 ± 1	0.06
E-cadherin	100 ± 2	92 ± 2	0.03	94 ± 2	0.21	99 ± 1	0.49
p70-S6K1	100 ± 1	93 ± 1	0.002	98 ± 1	0.06	99 ± 1	0.14
Akt	100 ± 5	71 ± 6	0.004	88 ± 3	0.04	99 ± 5	0.41
eEF2K	100 ± 3	85 ± 2	0.004	96 ± 4	0.37	96 ± 4	0.29
HSP27	100 ± 1	82 ± 3	0.0016	105 ± 4	0.021	119 ± 2	0.0009
HSP70	100 ± 1	91 ± 1	0.0016	97 ± 2	0.16	99 ± 1	0.38
MSH6	100 ± 2	89 ± 2	0.008	96 ± 2	0.02	95 ± 1	0.04
cJun	100 ± 2	94 ± 1	0.02	102 ± 1	0.49	100 ± 1	0.21
Merlin	100 ± 2	91 ± 3	0.034	105 ± 0.5	0.014	105 ± 1	0.04

Values show the level of expression of each protein where normoxia values are set to 100% and OIR, Arg-Gln dipeptide, and DHA values are relative to normoxic values. OIR pups treated with the Arg-Gln dipeptide or DHA (from P12 to P17) return expression levels of these proteins toward normoxic levels. The proteins modulated primarily by the dipeptide are shown in *green*. The proteins influenced most by DHA supplementation are shown in *blue*. The proteins similarly influenced by the dipeptide or DHA oral feeding are shown in *beige*. Fc fragment of IgG receptor 1b (IGFR1b), microtubule associated protein 1 light chain 3 alpha (LC3A), phosphoribosylaminoimidazole carboxylase and phosphoribosylaminoimidazolesuccinocarboxamide synthase (PAICS), replication protein A2 (RPA2), x-rayrepair cross complementing 1 (XRCC1), Jun kinase 2 (JNK2), ataxia telangiectasia mutated serine/threonine kinase (ATM), insulin receptor b (IR-b), programmed cell death 4 (Pcd4), phosphatidylinositol-4,5-bisphosphate 3-kinase (PI3K), AXL receptor tyrosine kinase (Axl), b-cell lymphoma-extra large (Bcl-xl), MAP kinase interacting serine/threonine kinase 1 (Mnk1), WD repeat domain phosphoinositide interacting 2 (WIPI2), ribosomal protein S6 kinase B1 (p70-S6K1), protein kinase B (Akt), eukaryotic elongation factor 2 kinase (eEF2K), heat shock protein 27 (HSP27), heat shock protein 70 (HSP70), Muts homology 6 (MSH6), Jun proteo-oncogene, AP-1 transcription factor subunit (c-Jun).

to that seen in healthy normoxic pups that did not undergo the OIR model.

However, some important caveats need to be considered. Vaso-obliteration and neovascularization were similarly prevented by Arg-Gln and DHA, but vascular density was restored only by Arg-Gln. These differences in the effects of Arg-Gln and of DHA are likely not due to differences in the levels of retinal DHA or NPD1, as levels were higher in the DHA-treated pups compared to the dipeptide-treated mice. This also suggests that

the beneficial effects of the dipeptide cannot be exclusively due to the changes in DHA and NPD1. While we do not have a mechanism accounting for the increase in capillary regrowth in the dipeptide-treated mice, our results would suggest that these events are independent of changes in LCPUFA and NPD1.

Interestingly, NPD1 is increased in the retina of OIR pups treated with the vehicle, compared to normoxia. This highlights the role of NPD1 production as an adaptive response of the retina to stress. NPD1 biosynthesis is promptly increased

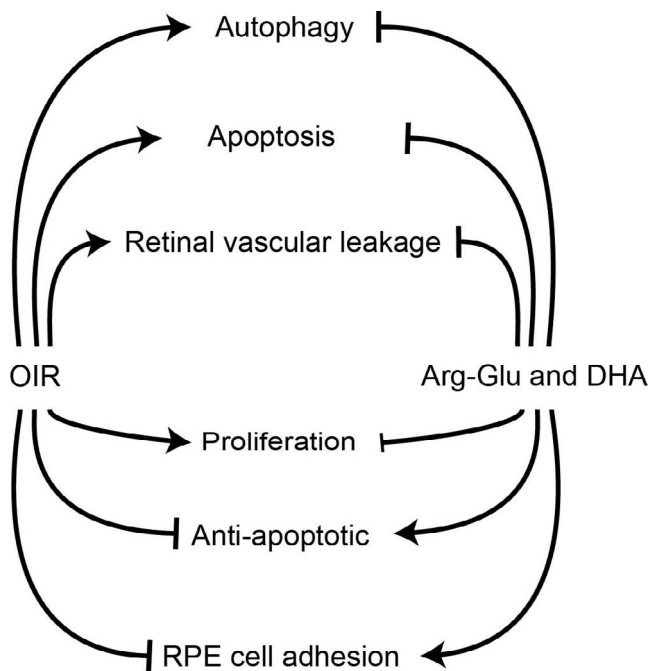


FIGURE 7. Schematic representation of impact of dipeptide treatment on OIR mouse model. Pups undergoing the OIR model showed increased levels of proteins associated with apoptosis, autophagy and permeability, and reductions in proteins that are needed for RPE cell adherence compared to pups maintained in room air. Gavage treatment of OIR mice with the Arg-Gln dipeptide stimulates retinal anti-apoptosis proteins and returned autophagy proteins and proteins promoting RPE cell adhesion toward levels observed in normoxia.

in response to oxidative stress,⁴⁸ protein misfolding,⁴⁹ and ischemia-reperfusion.⁵⁰ NPD1 is considered a protective protein made on demand in early stages of neural injury and one of the first defenses active when cell homeostasis is threatened by neurodegeneration. Thus, it is not surprising the neural retina in the current model of oxygen-induced injury shows increased levels of NPD1.

We show that proteins involved in apoptosis, retinal vascular leakage, and proliferation are expressed to a higher level in retinas of OIR pups, and supplementation with our test agents corrected these abnormalities. Our studies would suggest that possible mechanisms mediating the beneficial effects the dipeptide Arg-Gln and the accompanying restoration of endogenous DHA and NPD1 levels include the restoration of crucial signaling pathways that are adversely impacted by the OIR model. As shown in the schematic in Figure 7, the OIR model induces proteins that mediate proliferation (IGF-1Rb and IR-b) as well as mediate apoptosis (JNK2, programmed cell death protein 4, RPA32, and BIM). This is likely due to the rapid remodeling that is seen in this model. The OIR model also increases LC3A and proteins associated with vascular leakage (connexin-43 and serine-protein kinase ATM).

Both Arg-Gln dipeptide treatment and DHA treatment resulted in a reversal of many of the OIR-modulated signaling pathways (Figs. 6A, 6B), including the key proteins HSP27 and merlin. Differences in the proteomic data obtained from the dipeptide- and DHA-treated pups may explain aspects of the unique responses in these experimental cohorts.

The signaling proteins upregulated by DHA primarily include (1) Leber congenital amaurosis 3 (LC3A), critical for protein transport from the inner segment to the outer segment of photoreceptors, which if lost or defective triggers photorecep-

tor apoptosis⁵¹; (2) PAICS, a key enzyme involved in the de novo purine biosynthetic pathway⁵²; and (3) replication protein A (RPA) 32, a heterotrimeric single-stranded DNA binding complex with a critical role in replication and DNA repair.⁵³ In addition, DHA treatment increased caveolin-1 levels.

Two proteins were specifically reduced by DHA treatment, p70-S6K1 and E-cadherin. Protein kinase p70-S6K1 is regulated in response to cytokines, nutrients, and growth factors. It phosphorylates key cytoplasmic and nuclear substrates involved in the regulation of protein synthesis, cell cycle, cell growth, and survival.⁵⁴ Expression of E-cadherin, a well-known growth and invasion suppressor, was decreased. Collectively these findings support a role for DHA in mediating retinal remodeling and in reversing OIR-modulated signaling pathways.

Supplementation of the Arg-Gln dipeptide specifically modulated IGF and Src signaling.⁵⁵ The IGF-1R pathway influences vascular remodeling in part by mediating the activation of prosurvival pathways.⁵⁶ The selective effect of the dipeptide on promoting capillary regrowth may be mediated by improved IGF signaling as previously shown.^{26,57-63} Change in connexin-43 gap junction intercellular communication is an early event in angiogenesis.⁶⁴ Changes in caveolin-1-enriched microdomains involve Axl with lipid rafts⁶⁵ and imply that the dipeptide may modulate aspects of vascular hemostasis⁶⁶ also critical to the process of vascularization. Another protein, Bcl-xl, which plays an important role in the crosstalk between autophagy and apoptosis, was restored from low levels in the OIR retinas to levels associated with normoxia following dipeptide treatment.⁶⁷ Mnk1, a modulator of HIF1a and cell migration, was altered in OIR retinas with levels returning toward normoxia by the dipeptide treatment.⁶⁸ WIPI2, a critical protein in regulation of autophagy, was reduced following OIR but was restored toward normoxia by the dipeptide treatment.⁶⁹

In summary, oral administration of Arg-Gln is associated with increases in endogenous retinal DHA and NPD1 production. However, the beneficial effect observed with use of the dipeptide cannot be explained solely on the increase in DHA or NPD1, as exogenous administration of DHA did not result in increased capillary regrowth. This important difference suggests that dipeptide treatment likely modulates unique signaling pathways that are not influenced by exogenous DHA supplementation. Thus, our findings suggest that oral treatment with the dipeptide Arg-Gln to premature infants may represent a safe and highly beneficial therapy for prevention and treatment of ROP.

Acknowledgments

Supported by National Institutes of Health Grants R01EY0126001, R01EY007739, R01HL110170, R01DK090730 (MBG); Research to Prevent Blindness NIH EY005121 (NGB), unrestricted grant awarded to the Department of Ophthalmology at Indiana University-Purdue University-Indiana; NCI#CA16672 supporting the Reverse Phase Protein Array Core Facility.

Disclosure: L.C. Shaw, None; S. Li Calzi, None; N. Li, None; L. Moldovan, None; N. Sengupta-Caballero, None; J.L. Quigley, None; M. Ivan, None; B. Jun, None; N.G. Bazan, None; M.E. Boulton, None; J. Busik, None; J. Neu, None; M.B. Grant, None

References

- Liegl R, Hellstrom A, Smith LE. Retinopathy of prematurity: the need for prevention. *Eye Brain*. 2016;8:91-102.
- Shohat M, Reisner SH, Krikler R, Nissenkorn I, Yassur Y, Ben-Sira I. Retinopathy of prematurity: incidence and risk factors. *Pediatrics*. 1983;72:159-163.

3. Furst P, Albers S, Stehle P. Dipeptides in clinical nutrition. *Proc Nutr Soc.* 1990;49:343-359.
4. Furst P, Albers S, Stehle P. Glutamine-containing dipeptides in parenteral nutrition. *JPEN J Parenter Enteral Nutr.* 1990;14:118S-124S.
5. Neu J, Afzal A, Pan H, et al. The dipeptide Arg-Gln inhibits retinal neovascularization in the mouse model of oxygen-induced retinopathy. *Invest Ophthalmol Vis Sci.* 2006;47:3151-3155.
6. Vaughn P, Thomas P, Clark R, Neu J. Enteral glutamine supplementation and morbidity in low birth weight infants. *J Pediatr.* 2003;142:662-668.
7. Wu G, Jaeger LA, Bazer FW, Rhoads JM. Arginine deficiency in preterm infants: biochemical mechanisms and nutritional implications. *J Nutr Biochem.* 2004;15:442-451.
8. Abcouwer SF, Marjon PL, Loper RK, Vander Jagt DL. Response of VEGF expression to amino acid deprivation and inducers of endoplasmic reticulum stress. *Invest Ophthalmol Vis Sci.* 2002;43:2791-2798.
9. Bobrovnikova-Marjon EV, Marjon PL, Barbash O, Vander Jagt DL, Abcouwer SF. Expression of angiogenic factors vascular endothelial growth factor and interleukin-8/CXCL8 is highly responsive to ambient glutamine availability: role of nuclear factor-kappaB and activating protein-1. *Cancer Res.* 2004;64:4858-4869.
10. Marjon PL, Bobrovnikova-Marjon EV, Abcouwer SF. Expression of the pro-angiogenic factors vascular endothelial growth factor and interleukin-8/CXCL8 by human breast carcinomas is responsive to nutrient deprivation and endoplasmic reticulum stress. *Mol Cancer.* 2004;3:4.
11. Poindexter BB, Ehrenkranz RA, Stoll BJ, et al. Parenteral glutamine supplementation does not reduce the risk of mortality or late-onset sepsis in extremely low birth weight infants. *Pediatrics.* 2004;113:1209-1215.
12. Amin HJ, Zamora SA, McMillan DD, et al. Arginine supplementation prevents necrotizing enterocolitis in the premature infant. *J Pediatr.* 2002;140:425-431.
13. Smith LE, Wesolowski E, McLellan A, et al. Oxygen-induced retinopathy in the mouse. *Invest Ophthalmol Vis Sci.* 1994;35:101-111.
14. Hasan A, Pokeza N, Shaw L, et al. The matricellular protein cysteine-rich protein 61 (CCN1/Cyr61) enhances physiological adaptation of retinal vessels and reduces pathological neovascularization associated with ischemic retinopathy. *J Biol Chem.* 2011;286:9542-9554.
15. Chan-Ling T, Page MP, Gardiner T, Baxter L, Rosinova E, Hughes S. Desmin ensheathment ratio as an indicator of vessel stability: evidence in normal development and in retinopathy of prematurity. *Am J Pathol.* 2004;165:1301-1313.
16. Chang KH, Chan-Ling T, McFarland EL, et al. IGF binding protein-3 regulates hematopoietic stem cell and endothelial precursor cell function during vascular development. *Proc Natl Acad Sci U S A.* 2007;104:10595-10600.
17. Wang Y, Botolin D, Xu J, et al. Regulation of hepatic fatty acid elongase and desaturase expression in diabetes and obesity. *J Lipid Res.* 2006;47:2028-2041.
18. Connor KM, Kroh NM, Dennison RJ, et al. Quantification of oxygen-induced retinopathy in the mouse: a model of vessel loss, vessel regrowth and pathological angiogenesis. *Nature.* 2009;4:1564-1573.
19. Niemoller TD, Stark DT, Bazan NG. Omega-3 fatty acid docosahexaenoic acid is the precursor of neuroprotectin D1 in the nervous system. *World Rev Nutr Diet.* 2009;99:46-54.
20. Mintz-Hittner HA, Kennedy KA, Chuang AZ, BEAT-ROP Cooperative Group. Efficacy of intravitreal bevacizumab for stage 3+ retinopathy of prematurity. *N Engl J Med.* 2011;364:603-615.
21. Sanghvi KP, Kabra NS, Padhi P, Singh U, Dash SK, Avasthi BS. Prophylactic propranolol for prevention of ROP and visual outcome at 1 year (PreROP trial). *Arch Dis Child Fetal Neonatal Ed.* 2017;102:F389-F394.
22. Hong YR, Kim YH, Kim SY, Nam GY, Cheon HJ, Lee SJ. Plasma concentrations of vascular endothelial growth factor in retinopathy of prematurity after intravitreal bevacizumab injection. *Retina.* 2015;35:1772-1777.
23. Patel RD, Blair MP, Shapiro MJ, Lichtenstein SJ. Significant treatment failure with intravitreal bevacizumab for retinopathy of prematurity. *Arch Ophthalmol.* 2012;130:801-802.
24. Chhablani J, Rani PK, Balakrishnan D, Jalali S. Unusual adverse choroidal reaction to intravitreal bevacizumab in aggressive posterior retinopathy of prematurity: the Indian Twin Cities ROP screening (ITCROPS) data base report number 7. *Semin Ophthalmol.* 2014;29:222-225.
25. Day S, Rainey AM, Harper CA III. Incomplete retinal vascularization after ranibizumab treatment of retinopathy of prematurity. *Ophthalmic Surg Lasers Imaging Retina.* 2017;48:75-78.
26. Lofqvist C, Niklasson A, Engstrom E, et al. A pharmacokinetic and dosing study of intravenous insulin-like growth factor-I and IGF-binding protein-3 complex to preterm infants. *Pediatr Res.* 2009;65:574-579.
27. Connor KM, SanGiovanni JP, Lofqvist C, et al. Increased dietary intake of omega-3-polyunsaturated fatty acids reduces pathological retinal angiogenesis. *Nat Med.* 2007;13:868-873.
28. Pawlik D, Lauterbach R, Turyk E. Fish-oil fat emulsion supplementation may reduce the risk of severe retinopathy in VLBW infants. *Pediatrics.* 2011;127:223-228.
29. Smithers LG, Gibson RA, McPhee A, Makrides M. Effect of long-chain polyunsaturated fatty acid supplementation of preterm infants on disease risk and neurodevelopment: a systematic review of randomized controlled trials. *Am J Clin Nutr.* 2008;87:912-920.
30. Anderson RE. Lipids of ocular tissues. IV. A comparison of the phospholipids from the retina of six mammalian species. *Exp Eye Res.* 1970;10:339-344.
31. O'Brien JS, Sampson EL. Fatty acid and fatty aldehyde composition of the major brain lipids in normal human gray matter, white matter, and myelin. *J Lipid Res.* 1965;6:545-551.
32. Fliesler SJ, Anderson RE. Chemistry and metabolism of lipids in the vertebrate retina. *Prog Lipid Res.* 1983;22:79-131.
33. Delton-Vandenbroucke I, Grammas P, Anderson RE. Polyunsaturated fatty acid metabolism in retinal and cerebral microvascular endothelial cells. *J Lipid Res.* 1997;38:147-159.
34. Qi X, Pay SL, Yan Y, et al. Systemic injection of RPE65-programmed bone marrow-derived cells prevents progression of chronic retinal degeneration. *Mol Ther.* 2017;25:917-927.
35. Rodriguez de Turco EB, Deretic D, Bazan NG, Papermaster DS. Post-Golgi vesicles cotransport docosahexaenoyl-phospholipids and rhodopsin during frog photoreceptor membrane biogenesis. *J Biol Chem.* 1997;272:10491-10497.
36. Niu SL, Mitchell DC, Litman BJ. Optimization of receptor-G protein coupling by bilayer lipid composition II: formation of metarhodopsin II-transducin complex. *J Biol Chem.* 2001;276:42807-42811.
37. Mitchell DC, Niu SL, Litman BJ. Optimization of receptor-G protein coupling by bilayer lipid composition I: kinetics of rhodopsin-transducin binding. *J Biol Chem.* 2001;276:42801-42806.
38. Miasoedov DV. Indications for cryodestruction of cancer of the rectum [in Russian]. *Klin Khir.* 1975;5-8.

39. Devynck MA, Rostin M, David-Duflho M, Montastruc JL. Neurohumoral factors and the vasomotor system [in French]. *Arch Mal Coeur Vaiss*. 1986;79:1824-1826.
40. Agbaga MP, Brush RS, Mandal MN, Henry K, Elliott MH, Anderson RE. Role of Stargardt-3 macular dystrophy protein (ELOVL4) in the biosynthesis of very long chain fatty acids. *Proc Natl Acad Sci U S A*. 2008;105:12843-12848.
41. Tikhonenko M, Lydic TA, Opreanu M, et al. N-3 polyunsaturated fatty acids prevent diabetic retinopathy by inhibition of retinal vascular damage and enhanced endothelial progenitor cell reparative function. *PLoS One*. 2013;8:e55177.
42. Tikhonenko M, Lydic TA, Wang Y, et al. Remodeling of retinal fatty acids in an animal model of diabetes: a decrease in long-chain polyunsaturated fatty acids is associated with a decrease in fatty acid elongases Elovl2 and Elovl4. *Diabetes*. 2010;59:219-227.
43. Yonekawa Y, Miller JW, Kim IK. Age-related macular degeneration: advances in management and diagnosis. *J Clin Med*. 2015;4:343-359.
44. Le HD, Meisel JA, de Meijer VE, Gura KM, Puder M. The essentiality of arachidonic acid and docosahexaenoic acid. *Prostaglandins Leukot Essent Fatty Acids*. 2009;81:165-170.
45. Garcia-Layana A, Recalde S, Alaman AS, Robredo PF. Effects of lutein and docosahexaenoic acid supplementation on macular pigment optical density in a randomized controlled trial. *Nutrients*. 2013;5:543-551.
46. Dawczynski J, Jentsch S, Schweitzer D, Hammer M, Lang GE, Strobel J. Long term effects of lutein, zeaxanthin and omega-3-LCPUFAs supplementation on optical density of macular pigment in AMD patients: the LUTEGA study. *Graefes Arch Clin Exp Ophthalmol*. 2013;251:2711-2723.
47. Lien EL. Toxicology and safety of DHA. *Prostaglandins Leukot Essent Fatty Acids*. 2009;81:125-132.
48. Mukherjee PK, Marcheselli VL, Serhan CN, Bazan NG. Neuroprotectin D1: a docosahexaenoic acid-derived docosatriene protects human retinal pigment epithelial cells from oxidative stress. *Proc Natl Acad Sci U S A*. 2004;101:8491-8496.
49. Calandria JM, Mukherjee PK, de Rivero Vaccari JC, Zhu M, Petasis NA, Bazan NG. Ataxin-1 poly(Q)-induced proteotoxic stress and apoptosis are attenuated in neural cells by docosahexaenoic acid-derived neuroprotectin D1. *J Biol Chem*. 2012;287:23726-23739.
50. Chisholm JW, Hong J, Mills SA, Lawn RM. The LXR ligand T0901317 induces severe lipogenesis in the db/db diabetic mouse. *J Lipid Res*. 2003;44:2039-2048.
51. Subczynski W, Lukiewicz S. Electron spin resonance studies on aqueous methylene blue solutions. *Folia Histochem Cytochem (Krakow)*. 1973;11:41-49.
52. Dillard CJ, Tappel AL. Fluorescent products from reaction of peroxidizing polyunsaturated fatty acids with phosphatidyl ethanolamine and phenylalanine. *Lipids*. 1973;8:183-189.
53. Healey LA, Wilske KR, Webb DR, Sumida SS. Letter: Transfer factor in adult rheumatoid arthritis. *Lancet*. 1974;2:160.
54. Rosner M, Schipany K, Hengstschlager M. p70 S6K1 nuclear localization depends on its mTOR-mediated phosphorylation at T389, but not on its kinase activity towards S6. *Amino Acids*. 2012;42:2251-2256.
55. Min HY, Yun HJ, Lee JS, et al. Targeting the insulin-like growth factor receptor and Src signaling network for the treatment of non-small cell lung cancer. *Mol Cancer*. 2015;14:113.
56. Dziadziuszko R, Camidge DR, Hirsch FR. The insulin-like growth factor pathway in lung cancer. *J Thorac Oncol*. 2008;3:815-818.
57. Hellstrom A, Perruzzi C, Ju M, et al. Low IGF-I suppresses VEGF-survival signaling in retinal endothelial cells: direct correlation with clinical retinopathy of prematurity. *Proc Natl Acad Sci U S A*. 2001;98:5804-5808.
58. Liegl R, Lofqvist C, Hellstrom A, Smith LE. IGF-1 in retinopathy of prematurity, a CNS neurovascular disease. *Early Hum Dev*. 2016;102:13-19.
59. Hellstrom A, Ley D, Hansen-Pupp I, et al. Role of insulinlike growth factor 1 in fetal development and in the early postnatal life of premature infants. *Am J Perinatol*. 2016;33:1067-1071.
60. Stahl A, Hellstrom A, Smith LE. Insulin-like growth factor-1 and anti-vascular endothelial growth factor in retinopathy of prematurity: has the time come? *Neonatology*. 2014;106:254-260.
61. Ley D, Hansen-Pupp I, Niklasson A, et al. Longitudinal infusion of a complex of insulin-like growth factor-I and IGF-binding protein-3 in five preterm infants: pharmacokinetics and short-term safety. *Pediatr Res*. 2013;73:68-74.
62. Lofqvist C, Andersson E, Sigurdsson J, et al. Longitudinal postnatal weight and insulin-like growth factor I measurements in the prediction of retinopathy of prematurity. *Arch Ophthalmol*. 2006;124:1711-1718.
63. Hellstrom A, Engstrom E, Hard AL, et al. Postnatal serum insulin-like growth factor I deficiency is associated with retinopathy of prematurity and other complications of premature birth. *Pediatrics*. 2003;112:1016-1020.
64. Suarez S, Ballmer-Hofer K. VEGF transiently disrupts gap junctional communication in endothelial cells. *J Cell Sci*. 2001;114:1229-1235.
65. Laurance S, Aghourian MN, Jiva Lila Z, Lemarie CA, Blostein MD. Gas6-induced tissue factor expression in endothelial cells is mediated through caveolin-1-enriched microdomains. *J Thromb Haemost*. 2014;12:395-408.
66. Laurance S, Lemarie CA, Blostein MD. Growth arrest-specific gene 6 (gas6) and vascular hemostasis. *Adv Nutr*. 2012;3:196-203.
67. Zhou F, Yang Y, Xing D. Bcl-2 and Bcl-xL play important roles in the crosstalk between autophagy and apoptosis. *FEBS J*. 2011;278:403-413.
68. Proud CG. Mnks, eIF4E phosphorylation and cancer. *Biochim Biophys Acta*. 2015;1849:766-773.
69. Dooley HC, Razi M, Polson HE, Girardin SE, Wilson MI, Tooze SA. WIPI2 links LC3 conjugation with PI3P, autophagosome formation, and pathogen clearance by recruiting Atg12-5-16L1. *Mol Cell*. 2014;55:238-252.